A-posteriori Estimation of Random Uncertainty for the Reflection Type Q-factor Measurements

Darko Kajfez

Department of Electrical Engineering, University of Mississippi, University, MS, 38677
darko.kajfez@gmail.com

Abstract ─ A frequently used Q factor measurement procedure consists of determining the values of the input reflection coefficient vs. frequency with the use of a network analyzer, and processing the measured values with a data-fitting procedure to evaluate the location and the size of the corresponding Q-circle. That information is then used to compute the value of the loaded and unloaded Q factors and the coupling coefficient of the resonator being tested. This paper describes a novel method of post-processing the measured data, which also provides information on the uncertainty of the obtained results. Numerical examples show that this a-posteriori procedure can not only provide the uncertainty estimates but also improve the accuracy of results, even in the presence of a significant level of random measurement noise.

Index Terms ─ Least squares data fitting, measurement uncertainty, Q-circle, unloaded Q factor, Smith chart.

I. INTRODUCTION

The Q factors of microwave resonators are conveniently determined using network analyzers that can accurately measure the amplitude and phase of scattering parameters. The topic that will be discussed here is the Q factor measurement of microwave one-port resonators. In particular, the numerical processing of the measured values of the complex reflection coefficient Γ as a function of frequency will be described, with an emphasis on estimating the uncertainties of the loaded and unloaded Q factors due to small random errors that are inextricably present in a measured set of data.

When the reflection coefficient of a high-Q resonator is plotted on a Smith chart as a function of frequency, its path describes an almost-perfect circle [1]. By analyzing the size and orientation of the Q-circle, it is possible to determine the loaded Q_L and unloaded Q_0 factors [2]. The majority of Q-factor measurements are based on analyzing the measured scattering parameter data [3]. Some analysis methods utilize only the amplitude of the measured data [4]-[6]. The accuracy of results can be further improved by including the phase of the reflection coefficient as well, thus treating the reflection coefficient as a complex number. When numerical data of the reflection coefficient are available as a function of frequency, it becomes possible to least-squares fit these points to a theoretical prediction of the model, as was done in [7]-[9], in order to determine the loaded and unloaded Q factors with great precision.

The novelty of the data processing proposed here is that it compares the measured complex reflection coefficient data vs. frequency, with the data generated by the equivalent circuit model. Such comparison enables one to estimate the random uncertainty of the loaded and unloaded Q factors, as will be explained in Section IV.

The uncertainty of a scientific measurement consists of two parts: random uncertainty and systematic uncertainty. The systematic uncertainty is caused by the imperfections of the equipment used in measurements. The present paper does not deal with systematic uncertainty, but assumes that the measuring equipment provides reliable data. Instead, the paper addresses random uncertainty, which may be determined by numerical processing of the measured data.

In an attempt to measure as accurately as possible, it quickly becomes clear that it is impossible to repeat any measurement exactly. The problem becomes: how many decimal points can be considered reliable? For real numbers, the uncertainty is expressed with the standard deviation σ, which implies that by repeating the same measurement many times, about 67% of results will fall within the specified uncertainty [10].

As shown in Fig. 1, Γ_d, known as the detuned reflection coefficient, is the limiting value of Γ that would be reached when the frequency tends to infinity, or to zero. The point Γ_L is on the diametrically opposite side of the Q circle from Γ_d, and indicates the location of the loaded resonant frequency f_L.

To develop a consistent procedure for data processing, an equivalent circuit is postulated which approximates the behavior of complex reflection coefficient Γ as a function of frequency. An important step of data processing is to determine the center Γ_c, the diameter d of the Q-circle, and the two points on the circle, denoted Γ_L and Γ_d.

Submitted On: June 30, 2020
Accepted On: October 4, 2020

https://doi.org/10.47037/2020.ACES.J.351001

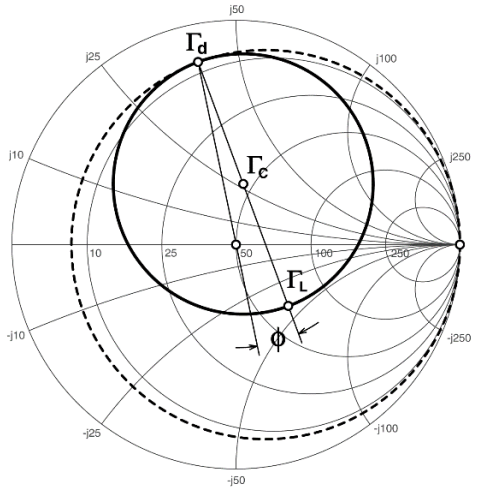

Fig. 1. Smith chart and the Q-circle (solid line).

II. EQUIVALENT CIRCUIT

The equivalent circuit, shown in Fig. 2, closely follows the one described in [9]. The "unloaded" resonator is represented by a parallel LCR resonant circuit described by the unloaded resonant frequency f_0, by the unloaded Q factor Q_0, and by the conductance G_0. The coupling discontinuity between the resonator and the transmission line leading to the network analyzer is modeled by the resistor R_s and the reactance X_s. The lossless transmission line has the characteristic impedance R_c and the phase delay θ. The network analyzer is represented by an ideal Thevenin source matched to the characteristic impedance of the transmission line. It is shown in [8] and [9] that for Q_0 values higher than 100, the values of R_s, X_s, and θ do not significantly influence the results of data fitting, as long as $R_s/R_c<<1$, $X_s/R_c<1$, and $\theta< 90°$.

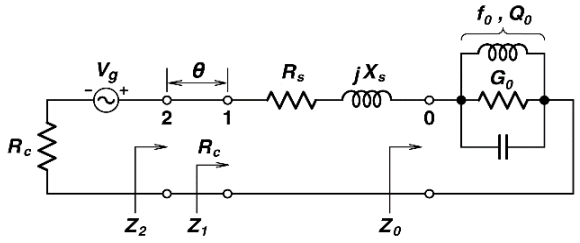

Fig. 2. The equivalent circuit with a parallel LCR resonator.

Within a limited frequency bandwidth, it is possible to describe the behavior of microwave networks with the help of lumped-element equivalent circuits. For that reason, the first step in measuring the Q factor is the so-called *pruning* process, where one selects a narrow range of frequencies within which the effect of resonance is most pronounced.

This typically happens around the minimum of the reflection coefficient magnitude. Within this range, the complex reflection coefficient on the Smith chart closely follows a circular path. It is prudent to select the pruned range such that no more than one-half of the circular arc is showing. Further away from the resonant frequency, the path departs more and more from an ideal circle, and the underlying assumptions are less and less justified. Thus, such data is best discarded, so that only a portion of the true Q circle is retained.

For the high-Q measurement, the "unloaded' part of the equivalent circuit, characterized by f_0, Q_0, and G_0, varies its impedance Z_0 much faster than the "external" part of the equivalent circuit, specified by R_s, X_s, and θ. For a resonator with a Q of 100, the pruned bandwidth is only about one percent wide. Within this narrow bandwidth, the behavior of the entire network can be understood more easily by assuming the values of R_s, X_s, and θ to be constant, independent of frequency. When the unloaded Q is much higher than 100, this assumption becomes even more justified.

Input impedance Z_0 of the unloaded resonator in Fig. 2 is represented by the LCR lumped-element resonant circuit, conveniently expressed as follows:

$$Z_0(\xi) = \frac{1}{G_0(1 + jQ_0\xi)}. \tag{1}$$

In the above, the frequency variable ξ is:

$$\xi = \left(\frac{f}{f_0} - \frac{f_0}{f} \right). \tag{2}$$

For numerical processing of data it is important to normalize the frequency, which was done above by dividing f by f_0. However, the exact value of unloaded resonant frequency f_0 is not known at the beginning of data processing. The practical solution is to normalize the frequency variable to the value f_n, the closest point to the center of the Smith chart. Within the narrow bandwidth in the vicinity of f_0, the approximate expression for the frequency variable becomes:

$$\xi \approx 2\frac{f - f_n}{f_n}. \tag{3}$$

The closest point to the center of the Smith chart is also the minimum of the reflection coefficient magnitude, as for instance in Fig. 3.

It is also convenient to normalize the impedances by dividing their values by the value of the characteristic impedance R_c. The normalized values will be denoted by lower-case symbols, like $r_s=R_s/R_c$, $x_s=X_s/R_c$, $r_0=1/(G_0R_c)$, *etc*.

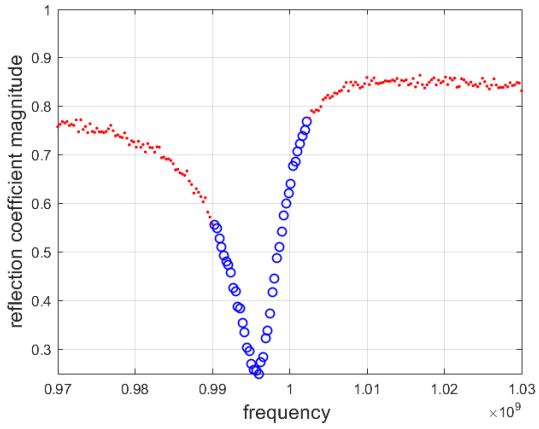

Fig. 3. Pruned region of frequencies (blue circles), and the discarded data (red dots). The random noise level is 1%.

When the measurement is performed through a known length of the transmission line, e.g., a coaxial connector, the measured impedance from port 2 has to be transformed to port 1, before applying the post-processing procedures to be described here. The corresponding measured reflection coefficient at port 1 is the following function of the normalized frequency ξ [9]:

$$\Gamma_1(\xi) = \Gamma_d + \frac{de^{j\gamma}}{jQ_L\xi + 1}. \tag{4}$$

Note that the phase angle γ above is not intended to have anything in common with the complex propagation constant. Also note that Q_L in (4) is the loaded Q factor and the frequency variable ξ is normalized to the loaded resonant frequency. Fortunately, the higher the value of Q_0 is, the smaller the difference between f_n and f_0, or between f_n and f_L.

In (4), d is the diameter of the Q-circle. At frequencies much higher or much lower than f_n, the value of ξ tends toward infinity and the reflection coefficient tends toward a limiting point Γ_d. Within the pruned range, the phase angle γ is:

$$\gamma = -2\tan^{-1}\left(\frac{x_s}{1+r_s}\right). \tag{5}$$

The coupling coefficient, denoted by the symbol κ, relates the loaded Q with the unloaded Q as follows:

$$Q_0 = Q_L(1+\kappa). \tag{6}$$

The behavior of the input reflection coefficient for the equivalent circuit in Fig. 2 can be conveniently described by the Möbius (also called bilinear) transformation:

$$\Gamma_1(\xi) = \frac{a_1\xi + a_2}{a_3\xi + 1}. \tag{7}$$

The graphical property of transformation (7) is to transform straight lines into circles, which makes it well suited for describing the measured Q-circles. The three complex constants a_1 to a_3 in (7) specify a continuous analytic function which approximates the behavior of the measured data in a least-squares sense. The details of determining the three complex coefficients from the set of measured reflection coefficient data can be found in [9]. Figure 4 is an exaggerated illustration of how a set of noisy data is approximated by a smooth circular arc, defined by (7).

The a-posteriori procedure proposed here starts after the elements of the equivalent circuit have been determined by some of the published procedures for the Q-factor measurement. The values of the elements in the equivalent circuit have been selected so that the input impedance, computed by the standard circuit analysis, very closely agrees with the actual impedance measured by the network analyzer. The uncertainty of the Q-factor measurement is then construed from the amount of the disagreement between the measured and the computed values, as will be explained in Section IV.

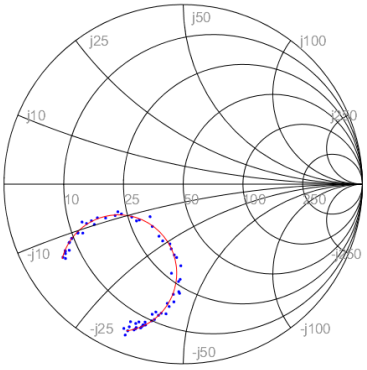

Fig. 4. Approximating noisy reflection coefficient data with the continuous function.

III. A-POSTERIORI ACCURACY IMPROVEMENTS

The knowledge of the element values in the equivalent circuit makes it possible to estimate more accurately the unloaded resonant frequency f_0, and the unloaded Q factor Q_0. One starts with the measured values of the input reflection coefficient Γ_1 at port 1. Transforming the measured reflection coefficient into the corresponding (normalized) impedance z_1, one can subtract from it the known value of $z_s=r_s+jx_s$ to obtain the value of the (normalized) input impedance z_0 at port 0 as

a function of frequency:

$$z_0(\xi) = \frac{r_0}{1 + jQ_0\xi}, \tag{8}$$

where ξ is now normalized to the unloaded resonant frequency f_0. The corresponding reflection coefficient of the unloaded resonator is:

$$\Gamma_0(\xi) = \frac{z_0(\xi) - 1}{z_0(\xi) + 1}. \tag{9}$$

Therefore, the three coefficients in the Möbius transformation for Γ_0 are:

$$a_{01} = -j\frac{Q_0}{1+r_0};\ a_{02} = \frac{r_0 - 1}{1+r_0};\ a_{03} = j\frac{Q_0}{1+r_0}. \tag{10}$$

The unloaded reflection coefficient Γ_0 at port 0 now describes a circle centered on the real axis, as shown in Fig. 5. This plot has been created from the validation file "v14.txt," that was computed for the element values given in Table 1.

The value of r_0 follows from a_{02}. Furthermore, realizing that a_{01} is a complex conjugate of a_{03}, the more accurate value of Q_0 is found to be:

$$Q_0 = \frac{2}{1 - a_{02}}\sqrt{a_{01}a_{03}}. \tag{11}$$

The accurate value of the unloaded resonant frequency f_0 can be obtained from the knowledge of Γ_0 as a function of frequency. The resonance occurs where Γ_0 crosses the real axis. Using the analytic form (9) again, a simple interpolation provides a value of f_0 which perfectly agrees with the known value of the validation data file "v14.txt." It should be mentioned that an accurate knowledge of the unloaded Q factor and the unloaded resonant frequency is very important, for instance in measuring the permittivity of the homogeneous and inhomogeneous dielectric materials filling microwave cavities [12, 13].

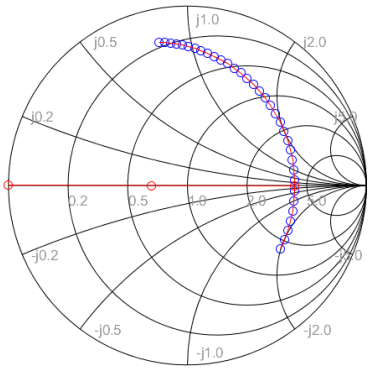

Fig. 5. The Smith chart showing the reflection coefficient Γ_0 of the unloaded resonator at port 0 (over coupled case).

IV. A-POSTERIORI DETERMINATION OF UNCERTAINTIES

After the values of reflection coefficient Γ have been measured, and the measured data have been processed to find the parameters of the equivalent circuit model, it becomes possible to compare the measured values of the reflection coefficient with the ones that the equivalent circuit predicts. The disagreement between the measured and the predicted values can be quantified by computing the standard deviation between the measured values of Γ and those predicted by the equivalent circuit. This way, each individual measured frequency point is checked to see how well it agrees with the postulated model.

The flowchart of the proposed procedure is summarized in Fig. 6. The starting point consists of the measured reflection coefficient values vs. frequency. They typically form three long columns of data: the frequency, the real part of Γ, and the imaginary part of Γ. The number of rows may vary from one hundred to more than one thousand. These are called the raw measured data.

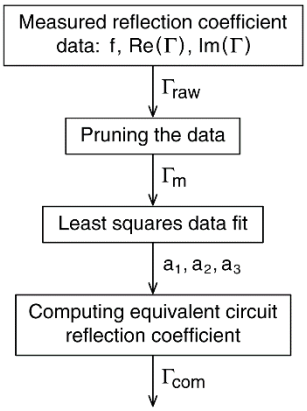

Fig. 6. The flowchart of the a-posteriori procedure.

The first step of data processing is the so-called *pruning*. The user is supposed to select a number of points on each side of the minimum of the reflection coefficient magnitude. For a reliable result, between 25 to 50 points are recommended. These are the measured data Γ_m that will be used for numerical processing. An example of pruning is illustrated in Fig. 3.

The second step of the procedure is to perform the least-squares data fit on a circle in the complex plane. The size and the position of the circle is described by three complex coefficients a_1 to a_3. These three coefficients describe the continuous function (7), which is represented by a solid line in Fig. 4.

The third step of data processing is to determine

the values of the equivalent circuit elements shown in Fig. 2. Afterwards, one can evaluate the (normalized) input impedance $z_2(\xi)$ at port 2. The input reflection coefficient is then obtained from z_2 as follows:

$$\Gamma_{com}(\xi)=\frac{z_2(\xi)-1}{z_2(\xi)+1}. \tag{12}$$

Now it becomes possible to statistically compare the equivalent circuit points $\Gamma_{com}(\xi)$ with the measured points $\Gamma_m(\xi)$, and estimate the uncertainty of the quantities of interest, like the unloaded Q factor, the coupling coefficient, *etc*.

A. Uncertainty of d

The diameter d of the Q-circle is important for determining the coupling coefficient κ. From (4), d is found as follows:

$$d(\xi)=\left|\left(jQ_L\xi+1\right)\left(\Gamma(\xi)-\Gamma_d\right)\right|. \tag{13}$$

The absolute value was used because d must be a real, positive number. For $\Gamma(\xi)$ one substitutes the actual measured points of the reflection coefficient within the pruned region. Although there is only one value of diameter d which fits the measured data in the least squares sense, $d(\xi)$ is formally represented above as a function of the frequency variable ξ. The results of (13) vary slightly as a function of frequency, because each measurement instrument has its uncertainty limits which we want to quantize here. This is accomplished by substituting the measured values $\Gamma(\xi)$ in the above equation, and evaluating the corresponding standard deviation σ(d) [10].

B. Uncertainty of Q_L

From (4) one obtains:

$$j\xi Q_L=\frac{de^{j\gamma}}{\Gamma_1(\xi)-\Gamma_d}-1. \tag{14}$$

Since Q_L is supposed to be a constant and real number, we need only the imaginary part of both sides of the equation. Then, by taking the derivative with respect to ξ we get:

$$Q_L(\xi)=-\mathrm{Im}\left(\frac{de^{j\gamma}}{\left(\Gamma_1(\xi)-\Gamma_d\right)^2}\cdot\frac{d\Gamma_1(\xi)}{d\xi}\right). \tag{15}$$

From (4) one realizes that the needed complex constant in the numerator is obtained when ξ is zero, namely: $de^{j\gamma}=\Gamma_1(0)-\Gamma_d$.

Although it would be possible to evaluate the error estimate of Q_L by performing numerical derivatives on the measured data of the reflection coefficient, more accurate results are obtained by taking the derivative of the continuous function (7):

$$Q_L(\xi)=-\mathrm{Im}\left(\frac{de^{j\gamma}}{\left(\Gamma_1(\xi)-\Gamma_d\right)^2}\cdot\frac{a_1-a_2a_3}{\left(a_3\xi+1\right)^2}\right). \tag{16}$$

By substituting the measured reflection coefficient data $\Gamma_1(\xi)$ in the above expression, one obtains an estimate of the standard deviation $\sigma(Q_L)$ [10].

C. Uncertainty of Q_0

From (8) and (9), it is possible to express Q_0 in terms of $\Gamma_0(\xi)$ as follows:

$$Q_0(\xi)=-\mathrm{Im}\left(\frac{2r_0}{\left(\Gamma_0(\xi)+1\right)^2}\cdot\frac{a_{01}-a_{02}a_{03}}{\left(a_{03}\xi+1\right)^2}\right). \tag{17}$$

The above expression provides the way to verify how well the measured values (after subtracting the coupling resistance and reactance) fit the circular behavior of the kind shown in Fig. 5. This is performed for all the pruned frequency points. The standard deviation with respect to the Q_0 value from (11) yields the estimated uncertainty $\sigma(Q_0)$.

D. Overall uncertainty U_0

The general measure of how well the measured data agree with the data computed from the equivalent circuit can be obtained by evaluating the standard deviation of their difference, expressed in percents:

$$U_0=100\cdot std\left(\Gamma_{m1}(\xi)-\Gamma_{com1}(\xi)\right). \tag{18}$$

E. Estimating the value of θ

Until now, the discussion of the a-posteriori procedure was based on the assumption that the measured reflection coefficient at port 2 was identical with the reflection coefficient at port 1, thus assuming the length θ of the transmission line to be zero. In an actual measurement with a network analyzer, the reference point is typically located at the input side of a coaxial connector, so that the remainder of the connector represents an additional section of the coaxial transmission line. For a small but finite length of the transmission line θ, the two reflection coefficients are related as:

$$\Gamma_2(\xi)=\Gamma_1(\xi)e^{-i2\theta}. \tag{19}$$

We know the measured values of $\Gamma_2(\xi)$ as function of frequency, but $\Gamma_1(\xi)$ is rotated on the Smith chart by an unknown angle of 2θ. For a high-Q measurement, the angle θ can be assumed to be constant within the pruned range of frequencies. As long as the value of θ is smaller than one quarter wavelength (θ < 90°), it is possible to estimate its value by comparing the measured value of Γ_2 with the computed value of Γ_1, by using the known values of the (normalized) equivalent circuit elements r_s and x_s. It is convenient to use the detuned reflection

coefficient at port 1 for this purpose:

$$\Gamma_{d1} = \frac{r_s^2 + x_s^2 - 1 + j2x_s}{r_s^2 + x_s^2 + 1 + 2r_s}. \quad (20)$$

Reactance x_s is obtained from Γ_{d1} as follows:

$$x_s = \mathrm{Im}\left(\frac{1+\Gamma_{d1}}{1-\Gamma_{d1}}\right). \quad (21)$$

Resistance r_s is given by:

$$r_s = \frac{2}{d_s} - 1, \quad (22)$$

where d_s is the diameter of the coupling-loss circle (the dashed circle in Fig. 1):

$$d_s = \frac{1 - |\Gamma_{d1}|^2}{1 - (|\Gamma_{d1}|\cos\phi)}. \quad (23)$$

Now it becomes possible to compare the computed value Γ_{d1} at port 1 with the measured value Γ_{d2} at port 2, and find for what value of θ they best agree with each other. The difference to be minimized is:

$$\Delta\Gamma_d = \left|\Gamma_{d2} - \Gamma_{d1} e^{-j2\theta}\right|. \quad (24)$$

Figure 7 is an example of $\Delta\Gamma_d$ plotted as a function of θ. The validation file "v14k50.txt" for this example corresponds to the same equivalent circuit as the file "v14.txt" in Table 1, with a transmission line of the length θ=50° added to the equivalent circuit. It can be seen that the value of $\Delta\Gamma_d$ displays a minimum at the correct phase angle.

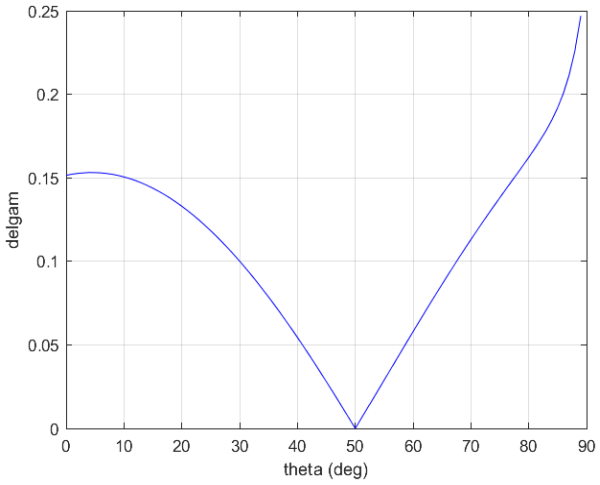

Fig. 7. Function $\Delta\Gamma_d$ vs. θ shows a minimum at the correct value θ=50°.

V. VALIDATION PROCEDURE

To validate the a-posteriori procedure, two different situations were investigated: a strongly coupled resonator with a coupling coefficient κ=2, and a loosely coupled case with κ=0.2. The loaded Q factor for the overcoupled case was chosen to be Q_L=100, and for the undercoupled case to be Q_L=1000. After selecting the element values of the equivalent circuit, the values of the complex reflection coefficient as a function of frequency have been computed by straightforward circuit analysis. Table 1 shows the assumed circuit element values of the two cases. The corresponding files were named "v14.txt" and "v13.txt." The ideal input reflection coefficients for each case were evaluated for 100 frequency points. Afterwards, random errors were superimposed on the real and imaginary parts of the reflection coefficients, for 21 gradually increasing levels.

Table 1: Element values of validation files

File name	Q_0	Q_L	κ	r_s	x_s	θ°
v14.txt	300	100	2	0.2	-1	0
v13.txt	1200	1000	0.2	0.2	0.8	0
v14k50.txt	300	100	2	0.2	-1	50

The Matlab® program Q0REFL from [9] was used to evaluate the starting values of Q_L and Q_0. These values were then analyzed by the a-posteriori procedure. As the validation data were generated from the known values of circuit elements, the actual values of Q_0 and Q_L were accurately known, and could be compared with a-posteriori estimates. The results are displayed in Figs. 8 and 9. The horizontal axes indicate the percent level of the random noise added to the data, and the vertical axes display the percent uncertainty levels estimated by the a-posteriori procedure (dashed lines). The actual percentage errors are shown by circular dots.

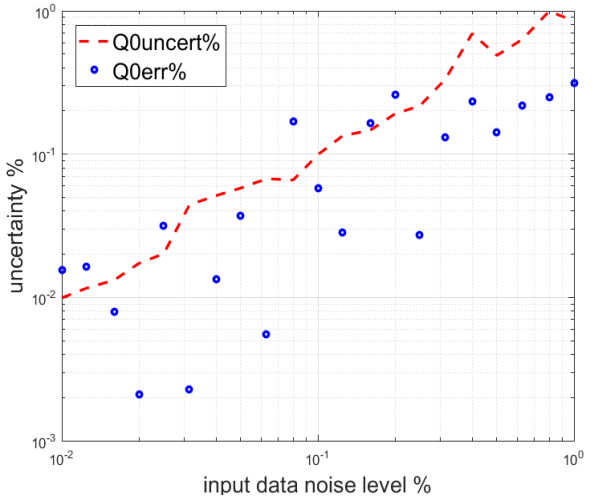

Fig. 8. Comparison of actual errors and estimated uncertainties (overcoupled case, file v14.txt).

Each of 21 randomly distorted "measured" data were manually pruned and individually processed in order to compare the estimated uncertainty with the actual error of the unloaded Q factor. As long as the actual error is smaller than the predicted uncertainty, the estimation is considered correct. Since we are dealing with random numbers, the majority (about two thirds) of the actual errors should come out to be smaller than predicted, but a few may happen to be larger. It can be seen that 15 out of 21 points fall clearly below the dashed line in Fig. 8, in agreement with the theoretically probable percentage.

The estimated uncertainties (dashed lines), when plotted in the log-log scale, display approximately linear dependence vs. the random noise that was added to the complex reflection coefficient. One can conclude from Fig. 8 that the estimated uncertainty of Q_0 will be smaller than 1% if the added noise is also about 1% (return loss of 20 dB).

When the resonator is undercoupled, the size of the Q-circle is relatively small, as for instance in the data file v13.txt, shown in Fig. 9. As the file name indicates, this particular input file had 0.01% random noise superimposed on the input data. The a-posteriori uncertainties for Q_L, Q_0, and κ are indicated by ± signs.

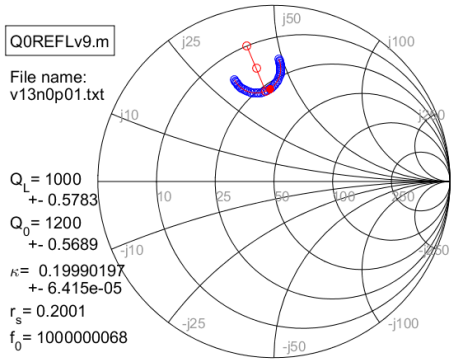

Fig. 9. Q-circle for the undercoupled case with κ=0.2.

Figure 10 compares the predicted uncertainties with the actual errors for the undercoupled case. Because of the small size of the Q-circles on the Smith chart, the relative accuracy of data fitting for the loosely coupled resonators comes out to be less accurate than for those that are overcoupled. It can be seen that the uncertainty will reach the value of 1% at a level of random noise 10 times smaller than in the overcoupled case. This happens at the random noise of 0.1%, (40 dB return loss). For such a low level of random noise, none of the actual errors happens to be larger than the uncertainty estimates.

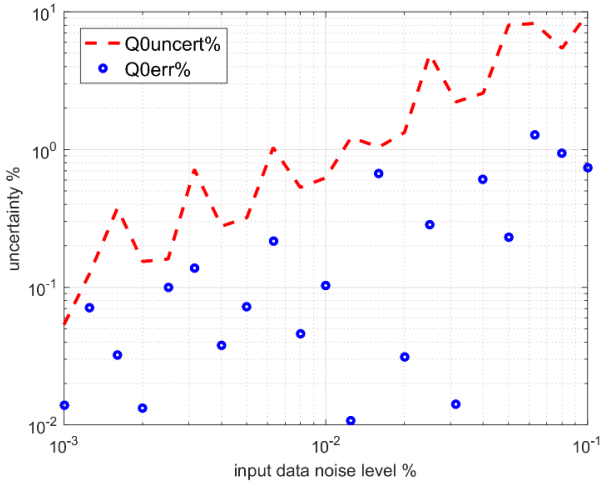

Fig. 10. Comparison of actual errors and estimated uncertainties for the unloaded Q factor (undercoupled case, file v13.txt).

VI. IMPLEMENTATION

The display of the new program may be seen in Fig. 11. The figure shows the results obtained for the input file "v14n1.txt," with an added noise level of 1%. Although such a high level of measured noise is not likely to happen in a typical measurement with a network analyzer, it can be seen that the improved value of Q_0 has been achieved with an error of only ±0.16%. This is within the estimated uncertainty of ±0.93 %.

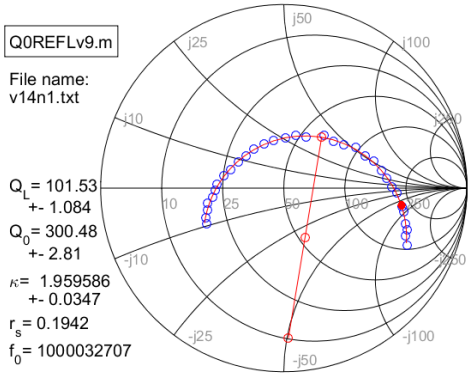

Fig. 11. The display of the program Q0REFLv9.

Another new result that the old version of the program Q0REFL was unable to provide is the unloaded resonant frequency f_0 (recall the interpolation associated with Fig. 5). In the example shown, the validation data file has been computed for the value of f_0=1.0 GHz,

whereas the recovered f_0 departs from that value at the fifth decimal place, in spite of the large noise added to the data.

The open source Matlab® program Q0REFLv9.m accepts the input data in Touchstone RI format (real and imaginary parts of the reflection coefficient), and it may be downloaded freely at [11].

VII. CONCLUSIONS

A systematic procedure for determining the random uncertainty of the reflection-type Q-factor measurement has been described. It consists of verifying how well the measured reflection coefficient fits an ideal circle on the Smith chart. The procedure can be summarized as follows.

An equivalent circuit consisting of 5 lumped circuit elements and of a lossless section of a transmission line is postulated, which is supposed to accurately simulate the measured reflection coefficient of a microwave resonator within the pruned frequency region. The a-posteriori processing of the measured data enables one to approximately determine the element values of the equivalent circuit and of the unloaded resonant frequency. Afterwards, one performs the computation of the input reflection coefficient for this equivalent circuit, and compares it statistically with the measured complex reflection coefficient. The procedure leads to explicit uncertainty estimates for the loaded and unloaded Q factors.

REFERENCES

[1] W. Altar, "Q circles - A means of analysis of resonant microwave systems," *Proc. IRE*, vol. 35, part I, pp. 355-361, Apr. 1947, Part II, pp. 478-484, May 1947.

[2] E. L. Ginzton, *Microwave Measurements*. New York: McGraw-Hill, 1957.

[3] A. Luiten, "Q factor measurements," in *Encyclopedia of RF and Microwave Engineering*. vol. 5, Kai Chang, Ed., New York, NY, USA, Wiley Science, pp. 3948-3964, 2005.

[4] Z. Ma and Y. Kobayashi, "Error analysis of the unloaded Q-factors of a transmission-type resonator measured by the insertion loss and the return loss method," *2002 IEEE MTT-S Digest*, pp. 1661-1664, 2002.

[5] T. Miura, "A proposal for standard to compare Q-factor evaluation accuracy of microwave resonator," *2006 MTT-S Internat. Microwave Symposium Digest*, pp. 1963-1966, 2006.

[6] R. Krolak and R. Fischerauer, "Q-factor estimation from the return loss of low-Q microwave resonators," *IEEE Trans. Microwave Theory Tech*., vol. 64, pp. 3797-3806, Nov. 2016.

[7] S. Shahid, J. A. R. Ball, C. G. Wells, and P. Wen, "Reflection type Q-factor measurement using standard least squares methods," *IET Microwave Antennas Propag*., vol. 5, pp. 426-432, 2011.

[8] D. Kajfez, *Q factor*. Oxford, MS, USA: Vector Forum, 1994.

[9] D. Kajfez, *Q Factor Measurements Using Matlab®*. Boston, MA, USA: Artech House, 2011.

[10] L. G. Parratt, *Probability and Experimental Errors in Science*. New York, NY, USA: John Wiley & Sons, 1961.

[11] https://egrove.olemiss.edu/engineering_software/1/

[12] R. Peter and G. Fischerauer, "Measurement of axially inhomogeneous permittivity distributions in resonant microwave cavities," *IEEE Trans. Microwave Theory Tech*., vol. 67, no. 6, pp. 2433-2442, June 2019.

[13] J. R. Sanchez, V. Nova, C. Bachiller, B. Villacampa, A. de la Rua, R. Kronberger, F. Penaranda-Foix, and V. E. Boria, "Characterization of nematic liquid crystal at microwave frequencies using split-cylinder resonator method," *IEEE Trans. Microwave Theory Tech.*, vol. 67, no. 7, pp. 2812-2820, July 2019.

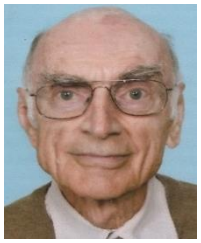

Darko Kajfež received the Dipl. Ing. degree in Electrical Engineering from the University of Ljubljana in 1953, and the Ph.D.degree from the University of California, Berkeley in 1967. Between 1950 and 1963 he worked with companies "IEV," "Rudi Čajavec,"and "Zavod za Avtomatizacijo" in Yugoslavia, primarily in microwave communications and radars. From 1963 to 1966 he was a Research Assistant at the Electronics Research Lab at University of California, Berkeley. Between 1967 and 2000 he was first Associate Professor and later Professor with the Department of Electrical Engineering, University of Mississippi in Oxford, MS. His research interests are in microwaves and antennas.